

Coupled Electrorotation of Polymer Microspheres for Microfluidic Sensing and Mixing

Clyde F. Wilson,[†] Mark I. Wallace,[†] Keisuke Morishima,[‡] Garth J. Simpson,[§] and Richard N. Zare^{*†}

Department of Chemistry, Stanford University, Stanford, California 94305-5080, Kanagawa Academy of Science and Technology (KAST), KSP West 614, 3-2-1 Sakado, Takatsu-ku, Kawasaki-shi, Kanagawa 213-0012, Japan, and Department of Chemistry, Purdue University, West Lafayette Indiana 47907-1393

We show that coupled electrorotation (CER) of microscopic particles using microfabricated electrodes can be used for localized sensing and mixing. The effective use of microelectromechanical systems and micro total analysis systems requires many types of control. These include the ability to (1) manipulate objects within microchannels by noncontact means, (2) mix fluids, and (3) sense local chemical parameters. Coupled electrorotation, in which the interactions between induced electric dipoles of adjacent particles lead to particle rotation, addresses aspects of all three challenges simultaneously. CER is a simple means of controlling the rotation of dielectric objects using homogeneous external radio frequency electric fields. CER is sensitive to several chemical and physical parameters such as the solution conductivity, pH, and viscosity. As a step toward integrating CER devices into microfluidic systems, a simple chip was designed to induce local mixing and to detect local changes in salt concentration, pH, and viscosity.

Electric fields have proven instrumental for the manipulation of microscale objects. Electrokinetic forces on a dielectric object in an electric field can be classified as producing either translational or rotational motion.¹ Translational motions can be induced by spatially homogeneous or inhomogeneous electric fields and are respectively termed electrophoresis and dielectrophoresis. Rotational motion is dependent on the formation of a dipole in the object to be rotated and the application of a torque to that dipole by an electric field. In electrorotation, a rotating electric field both induces dipole moments in particles and exerts a torque on the induced dipole moments, causing the particles to rotate. In coupled electrorotation (CER), the externally applied field is static and fixed in space. Dipoles are induced in two or more adjacent particles. A time delay exists in the buildup and decay of the dipole moments. Consequently, the electric field has in general two oscillating components offset in phase, one along the static field direction and one perpendicular to it. The sum of the two oscillating electric fields generates a rotating electric field that acts on each particle. The interaction between the two dipoles is

akin to the interaction between two bar magnets. In the case that one of the objects cannot rotate, dipoles are still induced and torques are still applied but only to the object that is free to rotate. The latter occurs when a microsphere is adjacent to a glass or polymer microstructure, for example.

Electrophoresis and dielectrophoresis have been the subject of extensive study for the manipulation of particles in microelectromechanical systems (MEMS) devices. For example, electrophoresis has been used for electroosmotic pumping² and chemical separations³ in MEMS devices. Dielectrophoresis has been used to trap and manipulate cells,^{4,5} viruses,⁶ and DNA.⁷ Traveling wave dielectrophoresis has also been used to separate and move particles in a microfluidic device.⁸

In contrast, the application of electrorotation to microfluidic analysis is relatively new. Historically, electrorotation has been used to characterize the properties of cells.^{9,10} Electrorotation has also been used to assess the viability of cells in real time, as it provides a measure of membrane integrity.¹¹ More recently, this application has been implemented in a MEMS device to characterize the cytoplasmic properties of cells.¹² Schnelle et al. have combined electrorotation in a quadrupole field with optical tweezers,¹³ allowing the simultaneous trapping and manipulation (translational and rotational) of particles.

The first demonstration of CER (two or more objects coupling to each other) was made by Teixeira-Pinto et al.¹⁴ in which *Euglena* and pseudopod fragments were observed to rotate spontaneously

- (2) SalimiMoosavi, H.; Tang, T.; Harrison, D. J. *J. Am. Chem. Soc.* **1997**, *119*, 8716–8717.
- (3) Manz, A.; Effenhauser, C. S.; Burggraf, N.; Harrison, D. J.; Seiler, K.; Fluri, K. *J. Micromech. Microeng.* **1994**, *4*, 257–265.
- (4) Jones, T. B. *Electromechanics of Particles*; Cambridge University Press: New York, 1996.
- (5) Mahaworasilpa, T. L.; Coster, H. G. L.; George, E. P. *Biochim. Biophys. Acta: Biomembr.* **1994**, *1193*, 118–126.
- (6) Morgan, H.; Green, N. G. *J. Electrostat.* **1997**, *42*, 279–293.
- (7) Asbury, C. L.; van den Engh, G. *Biophys. J.* **1998**, *74*, 1024–1030.
- (8) Cui, L.; Holmes, D.; Morgan, H. *Electrophoresis* **2001**, *22*, 3893–3901.
- (9) Arnold, W. M.; Zimmermann, U. Z. *Naturforsch. C: J. Biosci.* **1982**, *37*, 908–915.
- (10) Mischel, M.; Voss, A.; Pohl, H. A. *J. Biol. Phys.* **1992**, *10*, 223–226.
- (11) Goater, A. D.; Burt, J. P. H.; Pethig, R. *J. Phys. D: Appl. Phys.* **1997**, *33*, L65-L70.
- (12) Reichle, C.; Schnelle, T.; Müller, T.; Leya, T.; Fuhr, G. *Biochim. Biophys. Acta* **2000**, *1459*, 218–229.
- (13) Schnelle, T.; Müller, T.; Reichle, C.; Fuhr, G. *Appl. Phys. B: Lasers Opt.* **2000**, *70*, 267–274.
- (14) Teixeira-Pinto, A. A.; Kejelski, L. L., Jr.; Culter, J. L.; Heller, J. H. *Exp. Cell Res.* **1960**, *20*, 548.

* To whom correspondence should be addressed. E-mail: zare@stanford.edu.

[†] Stanford University.

[‡] Kanagawa Academy of Science and Technology.

[§] Purdue University.

(1) Goater, A. D.; Pethig, R. *Parasitology* **1998**, *117*, S177–S189.

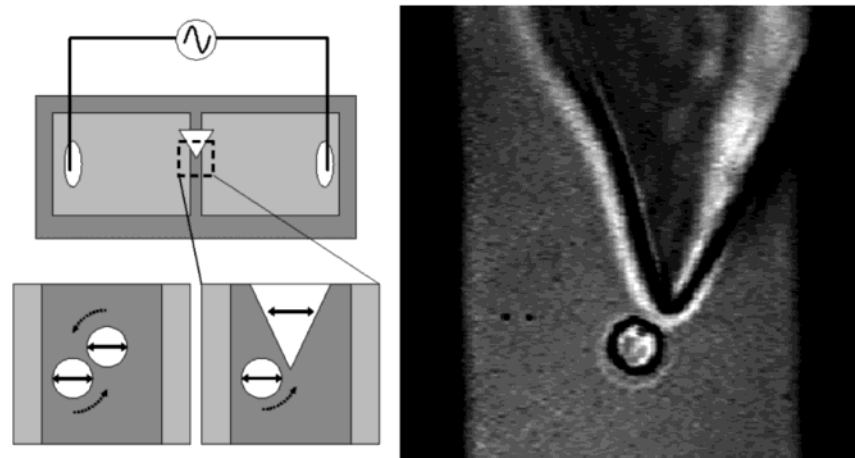


Figure 1. Microfabricated chips used to apply an electric field to two adjacent microspheres (for sensing experiments, not shown in this figure) or a microsphere adjacent to a PDMS corner (for mixing experiments). Wires connecting the function generator to the electrodes were attached to the latter using conductive epoxy (ovals). For a description of chip manufacture see text.

in strong rf fields when adjacent to a larger amoeba. Holzapfel et al.¹⁵ and Mahaworasilpa et al.¹⁶ presented theoretical formalisms to treat CER in an ac field. In recent work, we have combined CER with optical trapping and photopatterning to quantify rotation of submicrometer particles, fabricate microscopic “antigears,” and demonstrate the possibility of exploiting the registry of sphere rotation rates in performing local sensing.¹⁷ However, the instrumentation we used for inducing CER in this earlier work, in which microelectrodes were positioned using micromanipulators, was not ideally suited for direct incorporation into microfluidic devices. In addition, we demonstrated that a sealed pipet tip can induce a torque on a microsphere undergoing CER with another microsphere, but we had not used a stationary object to induce CER in a single microsphere.

Additional mechanisms to affect rotation of microscopic particles include all optical methods such as radiation pressure on microfabricated rotors,¹⁸ the trapping of birefringent particles,¹⁹ the use of Laguerre–Gaussian laser modes,²⁰ the use of optically trapped magnetic particles in rotating electromagnetic fields,²¹ and the fabrication of electrostatic or magnetic micromotors.²² Advantages of CER over these methods include the simplicity of the system needed to establish CER and the number of tasks that can be accomplished by CER simultaneously.

In this work, CER on a chip is demonstrated using microfabricated electrodes and optical tweezers to induce controlled rotation in individual pairs of microscopic objects. The coupled electrorotation rates of polystyrene microspheres were measured as a function of viscosity, NaCl concentration, and pH. The results

compared closely with theoretical models. The chip structures used to perform these measurements are well-suited for incorporation into more complex microfabricated devices. CER is achieved between a microsphere and an adjacent immobilized polymer microstructure. Application of CER for microfluidic mixing and sensing was also investigated.

EXPERIMENTAL SECTION

Particle rotation measurements were made using an apparatus similar to that described previously.¹⁷ Briefly, images were acquired using a Nikon Diaphot inverted microscope, collected by a silicon-intensified target (SIT, Hamamatsu C2400-08) camera, and recorded onto videotape. Dual optical trapping was achieved using a 985-nm MOPA diode laser (1 W, SDL model 5762-A6) split into its two polarization components. Each trap could be manipulated independently. A dichroic mirror allowed the introduction of both the optical trapping beams and the 488-nm excitation beam from an argon ion laser (SpectraPhysics Stabilite 2017). Microchips (see Figure 1) were constructed by sputtering gold (Hummer V Gold Sputter Coater, Technics, Inc., CA) onto glass coverslips (24 × 60 mm, No. 1, VWR Scientific, Inc., West Chester, PA) to a final thickness of ~100 nm. Photolithography was then used to etch a 10- μ m gap to separate the sputtered region into two equal halves, creating two electrodes of roughly equal size. Prior to sputtering, the glass coverslips were cleaned with methanol, 2-propanol, and acetone.

The chip was mounted over the oil immersion objective and a droplet (14–50 μ L) of 2- μ m latex spheres suspended in water was placed on the chip such that the drop was in contact with both gold electrodes. The latex spheres were Yellow-green carboxylate FluoSpheres (Molecular Probes, Eugene, OR) for sensing experiments and Polybead Carboxylate Microspheres (Polysciences, Inc., Warrington, PA) for mixing experiments. The latex spheres were diluted by a factor of ~100. The latex spheres from Molecular Probes are suspended in 2 mM sodium azide. We did not perform additional purification; the latex sphere solution used in the sensing experiments contained ~20 nM sodium azide. To achieve consistent results, the relative position of the microspheres in the optical traps was not changed during individual experiments.

(15) Holzapfel, C.; Vienken, J.; Zimmermann, U. *J. Membr. Biol.* **1982**, *67*, 13.

(16) Mahaworasilpa, T. L.; Coster, H. G. L.; George, E. P. *Biochim. Biophys. Acta: Biomembr.* **1996**, *1281*, 5–14.

(17) Simpson, G. J.; Wilson, C. F.; Gericke, K.; Zare, R. N. *ChemPhysChem* **2002**, *3*, 416–423.

(18) Ukita, H.; Kanehira, M. *IEEE J. Sel. Top. Quantum Electron.* **2002**, *8*, 111–117.

(19) Friese, M. E. J.; Nieminen, T. A.; Heckenberg, N. R.; Rubinsztein-Dunlop, H. *Nature* **1998**, *394*, 348–350.

(20) Paterson, L.; MacDonald, M. P.; Arlt, J.; Sibbett, W.; Bryant, P. E.; Dholakia, K. *Science* **2001**, *292*, 912–914.

(21) Sacconi, L.; Romano, G.; Ballerini, R.; Capitanio, M.; De Pas, M.; Giuntini, M.; Dunlap, D.; Finzi, L.; Pavone, F. S. *Opt. Lett.* **2001**, *26*, 1359–1361.

(22) Judy, J. W. *Smart Mater. Struct.* **2001**, *10*, 1115–1134.

139 Changes in the distance between microspheres results in signifi-
140 cant changes in rotation rate.

141 The effects of solution conductivity, pH, and viscosity on CER
142 were then measured. Experimental procedure was as follows: (1)
143 two microspheres were immobilized in the dual optical trap with
144 one microsphere (M1) positioned at the focal point of the
145 excitation laser, (2) M1 was partially photoaltered with focused
146 488-nm light for 0.1 s, (3) a 500-kHz, 60 kV cm⁻¹ electric field
147 sine wave was applied across the microsphere pair (see below)
148 after 3 min had passed from the time of placing the drop on the
149 chip to ensure uniform and minimal evaporation between trials,
150 and (4) LIF measurements were acquired for 1 min with wide-
151 field 488-nm excitation by passing the excitation beam through a
152 spinning disk diffuser. Microsphere photoalteration (bleaching)
153 allowed visualization of rotation.²³ The bleaching time for beads
154 was selected to be less than the time required for the microsphere
155 to undergo rotational diffusion by more than a few degrees. The
156 chip was rinsed three times with drops the same size as those
157 used in the experiments. Rinsing was done with the same solution
158 used in the following trial. Mixing experiments were performed
159 by replacing one microsphere with a poly(dimethylsiloxane)
160 (PDMS) wedge mounted between the electrodes. Drop sizes used
161 for the experiments were ~50 μL for mixing experiments, 30 μL
162 for pH measurements, and 14 μL for salt and viscosity measure-
163 ments. Experiments taking longer than a few minutes to perform
164 or those involving pH measurements were in general done with
165 larger drop volumes to minimize effects from drop evaporation.

166 The rf output from a Stanford Research Systems function
167 generator was coupled directly to the microelectrodes. Wires were
168 attached to the electrodes with conductive epoxy (Circuitworks
169 CW2400, Chemtronics, Kennesaw, GA). The use of 500 kHz
170 optimized sphere rotation and provided a slight dielectrophoretic
171 repulsion to minimize interference from stray microspheres
172 floating into the trapping region. Consistent with previous
173 findings,^{24–26} isolated, single spheres did not rotate under these
174 conditions, confirming that electroosmotic flow is unimportant in
175 these experiments.

176 Rotation rates did not change significantly over the time scales
177 used for data acquisition (i.e., a few minutes or less). Evaporation
178 of the droplet resulted in noticeable changes in the rotation rates
179 for longer times (between 15 min to well over 3 h, depending on
180 the droplet size).

181 Visualization of local mixing was achieved by adding 500-nm
182 tracer particles (Yellow-green carboxylate FluoSpheres, Molecular
183 Probes) to an aqueous solution of 2-μm spheres (described above).
184 In this solution, a 2-μm polystyrene microsphere is subject to a
185 500-kHz, 60 kV cm⁻¹ electric field sine wave while in close
186 proximity to a static PDMS structure. The PDMS structure was
187 a sharp corner made by simply cutting a piece of PDMS with a
188 razor blade and placing the corner on the gap between the
189 electrodes. The presence of this PDMS corner induced CER in
190 microspheres. Local fluid flow was visualized by direct observation
191 of the trajectories of individual tracer particles.

(23) Simpson, G. J.; Wohland, T.; Zare, R. N. *Nano Lett.* **2002**, *2*, 207–210.

(24) Grosse, C.; Shilov, V. N. *Colloids Surf. A* **1998**, *140*, 199.

(25) Grosse, C.; Shilov, V. N. *J. Phys. Chem.* **1996**, *100*, 1771–1778.

(26) Neu, B.; Georgieva, R.; Bäumlner, H.; Shilov, V. N.; Knippel, E.; Donath, E. *Colloids Surf. A* **1998**, *140*, 325.

THEORY 192

DEP and CER forces are principally determined by conductivity 193
in the surface layer of a particle.^{27–29} This surface layer describes 194
a thin three-dimensional shell containing the charged groups in 195
the solvent double layer, at the particle surface, and within a thin 196
layer below the particle surface that is accessible to solvent.³⁰ Upon 197
application of a locally homogeneous rf electric field, a dipole is 198
created within the particle. 199

Dielectrophoresis and electrorotation are related by the 200
respective real and imaginary components of the Claussius– 201
Mossotti factor in the equations describing the forces upon a 202
particle. For the case of an ideal sphere, the dielectric force is³¹ 203

$$F = 2\pi r^3 \epsilon_m \epsilon_0 \operatorname{Re}[f(\omega)] \nabla E^2 \quad (1)$$

For electrorotation, the torque is³¹ 204

$$\Gamma = -4\pi r^3 \epsilon_m \epsilon_0 \operatorname{Im}[f(\omega)] E^2 \quad (2)$$

where ϵ_m is the relative dielectric constant of the suspension 205
medium, ϵ_0 is the permittivity of free space, r is the particle radius, 206
 E is the amplitude of the driving field, and $f(\omega)$ is the Claussius– 207
Mossotti factor, dependent on ω , the angular frequency of the 208
field.³¹ 209

$$f(\omega) = (\epsilon_p^* - \epsilon_m^*) / (\epsilon_p^* + 2\epsilon_m^*) \quad (3)$$

Here ϵ_p^* and ϵ_m^* are the effective relative complex permittivities 210
of the particle and the medium. An effective permittivity can be 211
used to model the properties of a particle as a homogeneous 212
sphere with equivalent dielectric properties. A more accurate 213
description of microsphere properties should use a surface-layer 214
model of microsphere conductivity and permittivity.³⁰ 215

The relative complex permittivity is described by 216

$$\epsilon^* = \epsilon - i\sigma/\omega\epsilon_0 \quad (4)$$

where ϵ is the real relative permittivity and σ is the medium 217
conductivity. 218

Assuming a Stokes–Einstein model of the solution viscosity, 219
the angular velocity Ω for one particle in a pair of identical particles 220
subject to CER can be described by¹⁶ 221

$$\Omega = \frac{3\epsilon_m}{8\eta} E^2 \sin 2\theta \left[\frac{\operatorname{Im}[f(\omega)]}{4 - \operatorname{Re}[f(\omega)]} \right]. \quad (5)$$

Here, η is the viscosity of the solution medium, E is the applied 222
alternating external electric field, and θ is the angle between the 223
applied field and the vector connecting the centers of the two 224
particles. 225

(27) Fuhr, G.; Kuzmin, P. I. **1986**, *Biophys. J.* *50*, 789–795.

(28) Sauer, F. A.; Schlogl, R. W. In *Interactions between Electromagnetic Fields and Cells*; Chiabre, A., Nicolini, C., Schwan, H. P., Eds.; Plenum Press: New York, 1985; pp 203–251.

(29) Arnold, W. M.; Schwan, H. P.; Zimmermann, U. J. *Phys. Chem.* **1987**, *91*, 5093–5098.

(30) Maier, H. *Biophys. J.* **1997**, *73*, 1617–1626.

(31) Arnold, W. M.; Zimmermann, U. J. *Electrostat.* **1988**, *21*, 151–191.

226 For the case of two different spheres, the ratio of angular
 227 velocities becomes¹⁷

$$\frac{\Omega_A}{\Omega_B} \cong \frac{\text{Im}[f_A(\omega)]}{\text{Im}[f_B(\omega)]} \left(\frac{\text{Im}[f_B(\omega)] + (R_A/r)^3 \text{Im}[f_A(\omega)f_B(\omega)]}{\text{Im}[f_A(\omega)] + (R_B/r)^3 \text{Im}[f_A(\omega)f_B(\omega)]} \right) \quad (6)$$

228 where R is the radius of the sphere, r is the distance between the
 229 spheres, and A and B are subscripts that denote the two different
 230 spheres.

231 Describing the two particles in terms of equivalent homoge-
 232 neous spheres, and in the case of identical particles with frequency
 233 independent permittivities and conductivities, the real and imagi-
 234 nary parts of the Clausius–Mossotti factor become

$$\text{Re}[f(\omega)] = \frac{\sigma_p^2 + \sigma_p \sigma_m - 2\sigma_m^2 + \omega^2(\epsilon_p - \epsilon_m)(\epsilon_p - 2\epsilon_p)}{(\sigma_p + 2\sigma_m)^2 + \omega^2(\epsilon_p + 2\epsilon_m)^2} \quad (7)$$

$$\text{Im}[f(\omega)] = \frac{3\omega(\epsilon_m \sigma_p - \epsilon_p \sigma_m)}{(\sigma_p + 2\sigma_m)^2 + \omega^2(\epsilon_p + 2\epsilon_m)^2} \quad (8)$$

235 These equations follow from the theory of Lampa,³² describing
 236 the torque exerted by a rotating field on a sphere as described in
 237 the review of Arnold and Zimmerman.³¹ We substitute eqs 7 and
 238 8 into eq 5 to predict the variation in rotation rate with viscosity
 239 and salt concentration.

240 RESULTS AND DISCUSSION

241 The variation of microsphere angular velocity with solution
 242 viscosity is shown in Figure 2. The expected $1/\eta$ dependence of
 243 rotation rate is observed. The solid line in Figure 2 corresponds
 244 to a nonlinear least-squares fit of the data to a model describing
 245 CER in terms of two equivalent homogeneous spheres. Both the
 246 variation in solution conductivity and dielectric permittivity are
 247 taken into account.³³ Changes in permittivity are assumed to follow
 248 the Rayleigh model for the mixing of a two-component, one-phase
 249 system of dielectric materials;

$$\frac{\epsilon_{12} - 1}{\epsilon_{12} + 2} = \phi_1 \frac{\epsilon_1 - 1}{\epsilon_1 + 2} + \phi_2 \frac{\epsilon_2 - 1}{\epsilon_2 + 2} \quad (9)$$

250 where ϵ_m is the dielectric constant of the mixture; ϵ_1 , ϵ_2 , ϕ_1 , and
 251 ϕ_2 are respectively the dielectric constant and volume fraction of
 252 the two components. Under the conditions used for these
 253 experiments, a change in viscosity of $5 \times 10^{-4} \text{ kg m}^{-1} \text{ s}^{-1}$
 254 is detected as ethylene glycol is added to the aqueous solution until
 255 roughly one-quarter of the solution is ethylene glycol. The rotation
 256 rate continues to fall, but the ability to detect changes in viscosity
 257 falls off dramatically. Thus, the dynamic range for these measure-
 258 ments when used as a viscometer is within $\sim 40\%$ of the viscosity
 259 of water. Changing the experimental conditions, such as increas-
 260 ing the electric field strength, would increase the absolute CER
 261 rotation rate, thereby increasing the dynamic range over which
 262 viscosity can be measured.

(32) Lampa, A. *Wien. Ber. 2a* **1906**, *115*, 1659–1690.

(33) Tsierkezos, N. G.; Molinou, I. E. *J. Chem. Eng. Data* **1998**, *43*, 989–993.

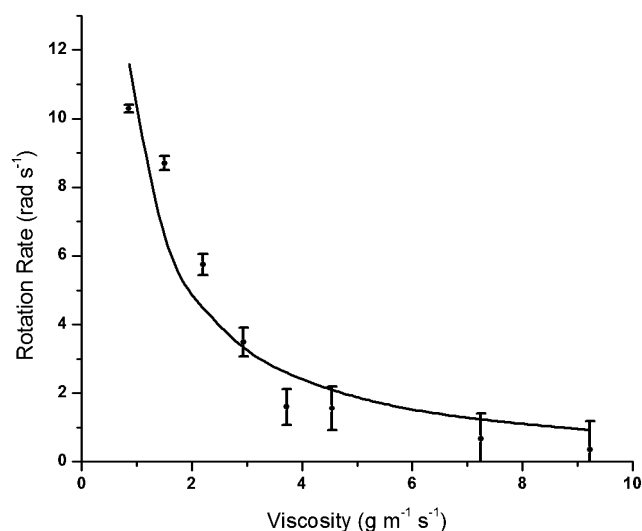


Figure 2. Variation of microsphere angular velocity with solution viscosity. The solid line corresponds to a nonlinear least-squares fit of the data to a model describing CER in terms of two equivalent homogeneous spheres. Variations in both solution conductivity and dielectric permittivity are taken into account. Fitting parameters: $E = \text{V m}^{-1}$, $\theta = \pi/4$, $\omega = 3.14 \times 10^6 \text{ rad s}^{-1}$, and $\sigma_m = 2.5 \times 10^{-4} \text{ S m}^{-1}$. A Rayleigh model of dielectric mixtures is used to describe the changes in solution permittivity. The fitted effective microsphere conductivity and relative permittivity are $\sigma_p = 6.2 \times 10^{-4} \text{ S m}^{-1}$ and $\epsilon_p = 18.8$, respectively.

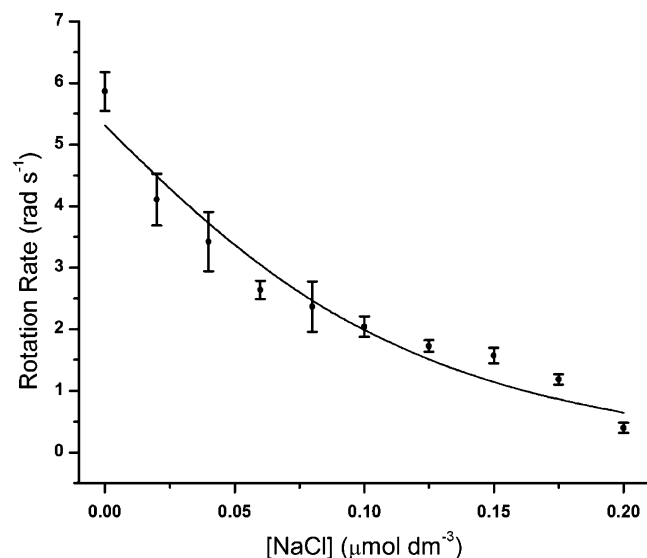


Figure 3. Variation of microsphere angular velocity with solution NaCl concentration. The solid line corresponds to a nonlinear least-squares fit of the data to a model describing CER in terms of two equivalent homogeneous spheres. Fitting parameters: $E = 10^5 \text{ V m}^{-1}$, $\theta = \pi/4$, $\omega = 3.14 \times 10^6 \text{ rad s}^{-1}$, and $\eta = 8.57 \times 10^{-4} \text{ kg m}^{-1} \text{ s}^{-1}$. The fitted effective microsphere conductivity and relative permittivity are $\sigma_p = 3.5 \times 10^{-4} \text{ S m}^{-1}$ and $\epsilon_p = 2.2$, respectively.

263 Figure 3 shows the dependence of rotation rate on the
 264 concentration of NaCl. Again, the solid line corresponds to a
 265 nonlinear least-squares fit using a model describing CER in terms
 266 of two equivalent spheres. Solution viscosity and dielectric
 267 permittivity are assumed constant. Under the conditions used for
 268 these experiments, changes in NaCl concentration of 40 nM were
 269 detected with a dynamic range of 0–200 nM in added salt
 270 corresponding to a conductivity range between 6 and 29 $\mu\text{S cm}^{-1}$.

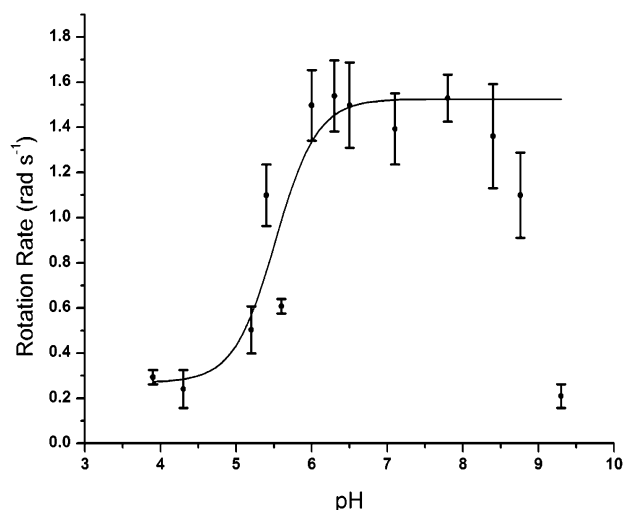


Figure 4. Variation of microsphere angular velocity with solution pH. The solid line corresponds to a nonlinear least-squares fit of the data to a sigmoid below pH 8. The pK_a of this fit is 5.5. The decrease in rotation rate at pH greater than 8 is caused by the change in conductivity as the ionic strength of the solution increases.

271 Measurable electrorotation and CER of polymer beads is not
 272 expected to occur under physiological conditions using reasonable
 273 field strengths. Nevertheless, electrorotation^{9–12} and CER^{14,15} of
 274 cells have been accomplished using sugar (or sugar alcohol)
 275 solutions of low ionic strength.

276 Figure 4 depicts the variation in rotation rate with solution pH.
 277 The value of the pH was varied by addition of 0.25 M NaOH to a
 278 5-mL unbuffered solution of microspheres whose initial pH was
 279 set at 3.9 by the addition of $\sim 0.1 \mu\text{L}$ of 37% HCl to a 225-mL stock
 280 solution. The conductivities for solutions similar to those used in
 281 the CER pH experiments were $55 \mu\text{S cm}^{-1}$ for pH 3.7, $29 \mu\text{S cm}^{-1}$
 282 for pH 4.4, and $32 \mu\text{S cm}^{-1}$ at pH 9.8. The conductivity was $24 \mu\text{S cm}^{-1}$
 283 for pH 5.2, 6.5, 7.3, and 8.6. The solid line in Figure 3
 284 describes a sigmoid fit to the pH changes below pH 8. This fit
 285 describes a simple mass balance between dissociation of protons
 286 from surface-bound carboxyl groups into the solution. The pK_a of
 287 this reaction is initially 5.5 ± 0.2 . This model does not take into
 288 account any dispersion in surface charge concentration. As the
 289 carboxy groups on the surface of the microsphere deprotonate,
 290 the increasing surface charge resists further deprotonation. The
 291 final carboxy groups to deprotonate have a pK_a of ~ 10 . The
 292 decrease in rotation rate at high pH is caused by the change in
 293 solution conductivity as the ionic strength of the solution in-
 294 creases. The high solution conductivities present when buffers
 295 are used to control pH reduce the rotation rate (similar to what
 296 is observed in Figure 3). Hence, buffers could not be used to
 297 stabilize the pH for these experiments and this may have
 298 contributed to the error in these measurements.

299 The ability to sense local variations in pH, conductivity, or salt
 300 concentration might be useful in work that requires specific
 301 conditions to function effectively. Maintaining optimum solubility
 302 of specific chemical species, optimizing chemical separation
 303 conditions, or ensuring that proper reaction conditions exist within
 304 a microfluidic system would be facilitated by improved local
 305 sensing capabilities. In addition, local sensing could provide
 306 improved information on how specific materials or surfaces within
 307 microfluidic devices alter the solution chemistry within the

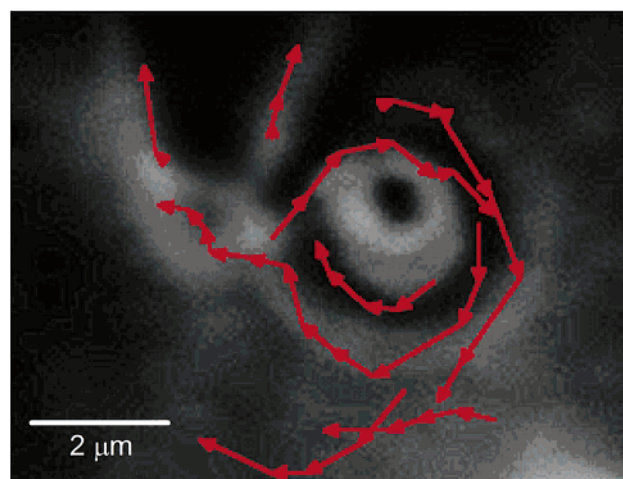


Figure 5. Visualization of local mixing around a polystyrene sphere in close proximity to a PDMS microstructure. Nine sample trajectories of fluorescent tracer particles are shown, demonstrating the local fluid flow around the rotating microsphere. Each vector represents a time interval of 33.3 ms. Bar is $2 \mu\text{m}$.

308 channels they contain (such as by leaching, adsorption, or
 309 absorption). Local sensing could also be an indicator for the
 310 effectiveness of cleaning or flushing processes. The simplicity of
 311 a CER microfluidic sensor also suggests that it might be used in
 312 a parallel manner to detect gradients in solution properties. Such
 313 a modification would only require the use of multiple optical traps.

314 The results depicted in Figure 5 demonstrate that CER can
 315 be used to affect mass transport and mixing at microscopic length
 316 scales, suggesting direct applications for mixing devices in chips.
 317 Fluid flow within a microfluidic device is in the low Reynolds
 318 number regime.^{34,35} As viscous rather than inertial effects control
 319 the fluid motion in this regime, mixing is dominated by diffusion.
 320 The ability to overcome the limitations of diffusional mixing and
 321 produce local turbulence is a key hurdle in the successful
 322 implementation of microfluidic devices. Alternative methods
 323 currently used to produce local microfluidic mixing include the
 324 use of charged surfaces,³⁶ t-junctions,³⁷ pulsatile flow,³⁸ acousto-
 325 fluidics,³⁹ optically driven microfabricated rotors,⁴⁰ or relief
 326 structures on the inner walls of the microchannel (e.g., ridges⁴¹
 327 or helical structures⁴²). CER may have several distinct advantages
 328 over many of these methods. For example, CER can be used to
 329 mix a localized region of fluid with dimensions smaller than 1
 330 μm . Physical contact is not needed between the mixing device
 331 and the chip as it is with microfabricated rotors. No special

(34) Purcell, E. M. *Am. J. Phys.* **1977**, *45*, 3–11.

(35) Brody, J. P.; Yager, P.; Goldstein, R. E.; Austin, R. H. *Biophys. J.* **1996**, *71*, 3430–3441.

(36) Kuxenok, O.; Yeomans, J. M.; Balazs, A. C. *Langmuir* **2001**, *17*, 7186–7190.

(37) Johnson, T. J.; Ross, D.; Locascio, L. E. *Anal. Chem.* **2002**, *74*, 45–51.

(38) Lee, B. S.; Kang, I. S.; Lim, H. C. *Int. J. Heat Mass Transfer* **1999**, *42*, 2571–2581.

(39) Rife, J. C.; Bell, M. I.; Horwitz, J. S.; Kabler, M. N.; Auyeung, R. C. Y.; Kim, W. J. *Sens. Actuators, A* **2000**, *86*, 135–140.

(40) Ukita, H.; Kanehira, M. *IEEE J. Sel. Top. Quantum Electron.* **2002**, *8*, 111–117.

(41) Stroock, A. D.; Dertinger, S. K. W.; Ajdari, A.; Mezic, I.; Stone, H. A.; Whitesides, G. M. *Science* **2002**, *295*, 647–651.

(42) Liu, R. H.; Stremmer, M. A.; Sharp, K. V.; Olsen, M. G.; Santiago, J. G.; Adrian, R. J.; Aref, H.; Beebe, D. J. *J. Microelectromech. Syst.* **2000**, *9*, 190–197.

332 processing is needed to create a microscopic mixer, and polymer
333 beads are readily available and easily used. Mixing can also be
334 turned on and off as required, as opposed to the mixing achieved
335 by a static structure. The positioning of the microsphere(s) is
336 readily adjustable, depending on the geometry of the applied
337 electric field and the range of movement of the optical trap holding
338 the microsphere(s). This flexibility allows some level of control
339 of the region to be mixed. A more quantitative investigation of
340 CER-induced local mixing could be achieved using particle image
341 velocimetry.

342 In summary, we have developed a microchip to optimize the
343 use of CER for sensing local changes in salt concentration,
344 viscosity, and pH (the three parameters that have the greatest
345 impact on the efficiency of CER). Changes in the rates of
346 microsphere CER were used to detect 40 nM changes in salt
347 concentration, $5 \times 10^{-4} \text{ kg m}^{-1} \text{ s}^{-1}$ changes in viscosity, and 0.2
348 pH unit changes in the region of the pK_a of the microsphere. The
349 microchip was also used to demonstrate microfluidic mixing

induced by CER between a microsphere and a PDMS microstruc- 350
ture. Taken together, CER is a versatile and simple tool that 351
simultaneously allows for the sensitive control of particle rotation 352
and microfluidic mixing and has applications in chemical sensing 353
within microfluidic systems. Its major drawback, at present, is the 354
need to operate CER at low ionic strength. 355

ACKNOWLEDGMENT 356

We thank Thorsten Wohland and Rebecca Whelan for their 357
assistance. C.F.W. expresses his thanks for a DuPont Pharma- 358
ceutical Graduate Fellowship and G.J.S. for a Pfizer and the Life 359
Sciences Research Foundation Postdoctoral Fellowship. This work 360
was supported by the National Science Foundation under NSF 361
00-119. 362

Received for review June 12, 2002. Accepted July 31, 363
2002. 364

AC0258599 365